PERIÓDICO TCHÊ QUÍMICA
ARTIGO ORIGINAL

CONFIABILIDADE DE INSTALAR FONTES DE ENERGIA TÉRMICA OCEÂNICA NA AMÉRICA DO SUL POR DIVERGÊNCIA DE TEMPERATURAS

RELIABILITY OF INSTALLING OCEANIC THERMAL ENERGY SOURCES AROUND SOUTH AMERICA BY DIVERGENCE OF TEMPERATURES

CONFIABILIDAD DE INSTALAR FUENTES DE ENERGIA TÉRMICA OCEÂNICA ALREDEDOR DE AMÉRICA DEL SUR POR DIVERGENCIA DE TEMPERATURAS

DÍEZ, César Manuel [1]*; ESTRADA, Carlos Manuel; VARAS Oscar H.; CAMARENA, Caroline Pamela; ATOC, Lari Jacson

[1] *Universidad Nacional de ingeniería. Facultad de Ingeniería Ambiental, Unidad de Investigación, Lima – Peru*

** Corresponding author*
e-mail: cdiezch@uni.edu.pe

Received 31 March 2021; received in revised form 06 February 2022; accepted 23 February 2022

RESUMO

Introdução: A população mundial tem crescido consideravelmente, aumentando a demanda por recursos primários, ou seja, água, energia elétrica; a geração de eletricidade renovável é a primeira aspiração do ser humano. A radiação do Sol é uma extensa fonte de energia sustentável, e essa radiação desaparece nas profundezas das águas oceânicas, tornando possível tirar proveito. **Objetivo:** O objetivo deste trabalho foi estabelecer um processo de absorção da radiação solar e convertê-la em energia, considerando um par de pontos de coordenadas geográficas, com grande diferencial de temperaturas nos oceanos da América do Sul para implementar máquinas térmicas. **Métodos:** Este trabalho processa dados de temperatura retirados do projeto *Tropical Atmosphere Ocean* (TAO), mantido pelo Laboratório Ambiental do Pacífico (PMEL) da Administração Nacional Oceânica e Atmosférica (NOAA). Os dados foram processados com Matlab 2009a Student Version. A temperatura da água implica o grau de intensidade da energia térmica do oceano. Então, este estudo usa dados de temperatura no mar ao redor da América do Sul para coletar energia térmica oceânica, o método da máquina de Carnot e gradientes de temperaturas. **Resultados e Discussão:** A área mais estável, anualmente, para instalar máquinas térmicas está a mais de 35° do Canal do Panamá e Trujillo para o meridiano oeste. Os valores mais fracos são encontrados perto de Quito (Equador); mas médio no Oceano Atlântico, sendo a melhor localização 15° a leste de Fortaleza de São José de Macapá (Brasil). Por outro lado, um gás real pode mudar sua velocidade de 40,0 m/s abaixo de 500,0 m do nível médio do mar (bmsl) até 650,0 m/s na superfície do mar, enquanto um gás artificial de 20,0 m/s até 400,0 m /s. **Conclusões:** Este estudo expõe que a energia captada nas costas, as mais quentes da América do Sul, traz energia suficiente para a população vizinha. Durante o tempo ENSO (El Niño Oscilação Sul), as águas do Oceano Pacífico aumentam sua energia térmica, de modo que o desempenho de saída será variado.

Palavras-chave: *Máquina de Carnot, Análise de dados, Processamento de dados, Energia térmica oceânica, Energia sustentável.*

ABSTRACT

Background: The world population has grown considerably, increasing the demand for primary resources, i.e., water, electricity; the generation of renewable electricity is the first aspiration of human beings. Radiation from the Sun is an extensive source of tenable energy, and this radiation fades in the depth of the ocean waters, making it possible to take benefit. **Aim:** The purpose of this work was to settle a process of absorbing Sun radiation and converting it into energy by considering a couple of geographical coordinate points, with a great differential of temperatures in the Oceans around South America, to implement thermal machines. **Methods:** This work processes temperature data taken from the Tropical Atmosphere Ocean (TAO) project, maintained by National Oceanic and Atmospheric Administration's (NOAA) Pacific Environmental Laboratory (PMEL). Data were processed with Matlab 2009a Student Version. Water temperature implies the intensity degree of ocean heat energy. So, this study takes temperature data at Sea around South America to glean oceanic thermal energy means the Carnot machine method and gradients of temperatures. **Results and Discussion**: The more stable area annually to install thermal machines are farther than 35° from Panama Canal and Trujillo to the west meridian. The weaker values are found near Quito (Equator); but medium in the Atlantic Ocean, being the better

Downloaded from www.periodico.tchequimica.com. © *The Author(s) 2022*
DOI: 10.52571/PTQ.v19.n40.2022.01_Chirinos_pgs_01_19.pdf.

location 15° to the East of Fortaleza de Sâo José de Macapá (Brazil). On the other side, a real gas could change its speed from 40.0 m/s below 500.0 m mean sea level (bmsl) up to 650.0 m/s at the Sea Surface, while an artificial gas from 20.0 m/s up to 400.0 m/s. **Conclusions:** This study exposes that the energy harvested on the coasts, the warmest of South America, brings sufficient energy to the neighboring population. During ENSO time (El Niño Southern Oscillation), the waters of the Pacific Ocean increase their thermal energy, so the output performance will be varied.

Keywords: *Carnot machine, Data analysis, Data process, Ocean thermal energy, Tenable energy.*

RESUMEN

Introducción: La población mundial ha crecido considerablemente, aumentando la demanda de recursos primarios, es decir, agua, electricidad; la generación de electricidad renovable es la primera aspiración del ser humano. La radiación del Sol es una fuente extensa de energía sostenible; y esta radiación se desvanece en la profundidad de las aguas oceánicas, haciendo posible aprovecharla. **Objetivo:** El propósito de este trabajo es establecer una forma de absorber la radiación solar y convertirla en energía, considerando un par de puntos de coordenadas geográficas, con un gran diferencial de temperatura alrededor de Sudamérica, para implementar máquinas térmicas. **Métodos:** Este trabajo procesa datos de temperatura tomados del proyecto Tropical Atmosphere Ocean (TAO), mantenido por el Laboratorio Ambiental del Pacífico (PMEL) de la Administración Nacional Oceánica y Atmosférica (NOAA). Los datos fueron procesados con Matlab 2009a Student Version. La temperatura del agua implica el grado de intensidad de la energía térmica del océano. Por lo tanto, este estudio toma datos de temperatura en el mar alrededor de América del Sur para obtener energía térmica oceánica mediante el método de la máquina de Carnot y gradientes de temperatura. **Resultados y Discusión:** Las áreas más estables, anualmente, para instalar máquinas se encuentran más alejadas de los 35° del Canal de Panamá y Trujillo hacia el meridiano oeste. Los valores más débiles se encuentran cerca de Quito (Ecuador); pero los medios en el Océano Atlántico, siendo el más óptimo a 15° al Este de Fortaleza de Sâo José de Macapá (Brazil). Por otro lado, un gas real podría cambiar su velocidad desde 40.0 m/s por debajo de 500.0 m del nivel del mar hasta 650.0 m/s en la superficie del mar, en tanto que, un gas artificial desde 20.0 m/s hasta 400.0 m/s. **Conclusiones:** Este estudio expone que la energía obtenida en las costas, las costas más cálidas de Sudamérica, aporta energía suficiente a la población vecina. Durante tiempo de ENOS (El Niño Oscilación del Sur), las aguas del Océano Pacífico aumentan su energía térmica, por lo que el rendimiento será variado.

Palabras clave: M*áquina de* Carnot*, análisis de Datos*, *Procesamiento de datos,* energía térmica Oceánica*, energía sostenible*.

1. INTRODUCTION:

Nowadays, renewable energies are sustainable forms of development for human beings (Hammar *et al.*, 2017). Radiations are emitted by the Sun (Resurreiçao *et al.*, 2011) as shortwave radiation (Emery and Pickard, 2007); this radiation generates a radiative imbalance, and 80% of its energy heats the Oceans (*Purkey and Johnson*, 2010), mainly to the western equatorial Pacific, it presents the warmest oceanic temperatures (McPhaden and Hayes, 1991). Then, the thermal declivity of the Ocean, in line with profoundness, may allow the building of thermal machines, because of its gradient, around South America, capturing this radiation to transform into thermal energy (Salen and Khan, 2017). Because global ocean heat affects considerably, primarily down the upper 0 – 700 m (Lyman and Johnson, 2013), there is an energy imbalance of the Earth associated with Global warming (Johnson, Mecking, Solyan, and Wijffels, 2007). El Niño and La Niña cause changes due to heat exchange (McPhaden *et al*., 2015), mainly in the equatorial Pacific (Meinen and McPhaden, 2000), cyclically year-to-year (McPhaden, Zebiak, and Glantz, 2006). Taking profit of this slope, there could be determined a hot reservoir of a thermal machine at the sea surface and a cold reservoir at upper waters, here 500 m bmsl (Faizal and Ahmed, 2017).

This work aims to map sites indicating how feasible the enforcement of a thermal plant that takes advantage of the ocean thermal energy around the South American Continent is. The first step was the presentation of the datasets, which means time series. The second step was the quantification of a Carnot machine efficiency considering these depths as reservoirs. The third step was the determination of gradients temperatures to obtain electrical energy vaporizing a gas from a colder temperature (Technische Universiteit Delft, 2021). And the last step was the calculation of the most probable average speed and Root Mean Square speed (rms, from now on) of two natural gases and two artificial gases to be used to supply turbines around these places. Also, this information may be useful to study energetical properties in the Ocean

Downloaded from www.periodico.tchequimica.com

around South America. To achieve this purpose, temperature data from the sea surface and at 500.0 m bmsl in the oceanic waters of South America to glean thermal energy were processed. Generally, the time series of thermal gradients fluctuate a lot, being difficult to control the motion of gases in any region, but far from the Panamanian and North of Peru littorals and near the coast of North Brazil, making these locations the best to install thermal energies. The natural gases, propane, and ammonium present major kinetical energies to supply a turbine in the Oceans, while artificial ones, R152a and R134a, present low kinetical energy for this purpose.

2. MATERIALS AND METHODS:

2.1. Data

To carry out this work, daily temperature data of sea surface temperatures and daily upper temperatures at 500 meters bmsl since 1980 of forty-four buoys were provided by the National Oceanography and Atmosphere Administration through the Pacific Marine Environment Laboratory, a property of the National Oceanic and Atmospheric Administration of the United States of America, in its Tropical Atmosphere Ocean project (TAO), which have the project Archive Tropical Moored Buoys Array divided into Moored Array for African-Asian-Australian Monsoon Analysis and Prediction RAMA, Prediction and Research Moored Array in the Tropical Atlantic (PIRATA), and Tropical Atmosphere Ocean / Triangle Transocean Network (TAO/TRITON) projects. Two geographic coordinates from these three networks are presented in this work; the TAO / TRITON – 9º N to 8º S / 95º W to 180º W - and the PIRATA – 21º N to 19º S / 23º W to 38º W - programs (PMEL-NOAA, 2015), see Figure 1. Missing data is not considered in the processes, and the software (Matlab 2009a Student version) omits space. These data were processed in several manuscripts such as The Upper Ocean heat balance (Cronin and McPhaden, 1997), On the Variability of Winds, Sea Surface Temperature, and Surface Layer Heat Content in the Pacific Ocean (McPhaden, Stanley and Hayes, 1991), Ocean Model Studies of Upper-Ocean Variability (Harrison and Craig, 1992).

2.2 Method

Three processes are presented, illustrating the most relevant graphic results. The first process, taking as sources the declivity of the reservoirs the temperatures of the Sea Surface and the upper waters at 500 m bmsl is the determination of the efficiency of a Carnot machine along the time, in order to earn the best production of a thermal machine, for an ideal case. As a second process, representation of Sea Surface temperatures and upper temperatures at 500 m bmsl and their corresponding gradient of temperatures are presented to establish limits where an adequate fluid may reach its maxima kinetic energy nearby their boiling points. As the last process, the kinetic behavior of four gases is performed; just R152a, R134a, ammonium, and propane (Bernardoni, Binotti, and Giostri, 2017); for the generation of fuel to supply thermal machines. The study of these four gases is presented to handle the more appropriate gas to supply turbines in South American waters; there will be stage three speeds analysis that depends on temperature, root mean square (RMS), average, and most probable speeds for the temperatures set by the reservoirs. Of course, energies should adapt to the hot reservoir, maximum kinetic result, and to the cold reservoir, stability (Etemadi *et al*., 2017).

2.2.1 Determination of energetic efficiency by Carnot Cycle

The early process quantifies a percentage of the total energy around the equatorial Pacific and Atlantic oceans, which would be possible to absorb to generate work via the Carnot method because it is the most competent thermodynamic manner for an ideal system. Its success will depend on its thermal efficiency, defined as the work that a thermal plant performs per cycle by the absorbed energy in each cycle (Rebhan, 2002). It means that this machine absorbs energy from the sea surface (Q_{ss}) at temperatures (T_{ss}) and discharges heat to a colder reservoir at 500 meters below the surface of the Ocean (Q_{500}) at a given temperature (T_{500}) (Semmari, 2012). Based on the first and second law of Thermodynamics, the definition of the Carnot machine, η, is given by Equation 1.

$$\eta = 1 - \frac{T_{500.0\,m}}{T_{ss}} \qquad \text{(Eq. 1)}$$

where:

$T_{500.0\,m}$: Temperature at 500.0 m bmsl.

T_{ss}: Sea surface temperature

2.2.2. Thermal gradients between the sea surface and upper temperatures

Downloaded from www.periodico.tchequimica.com

Another application besides the Carnot method; because it should be disadvantageous due to the low output of efficiency, is to harness the thermal inequality of the corresponding deepness, where the mentioned temperatures will limit the kinetic energy of a gas circulating inside this area to impulse a rotor of a turbine (Miller and Kusch, 1955). To appreciate differences between temperatures at the sea surface and at 500 m deep, time series of both temperatures will be presented by one side; and their correspondent gradients of temperatures, between T_{500} and T_{ss}, respect their depths, at 500.0 m bmsl and at Sea Surface, respectively, in time, see Equation 2:

$$\nabla T = \frac{T_{500.0\,m} - T_{ss}}{h_{500.0\,m} - h_{ss}} \qquad \text{(Eq. 2)}$$

where:

$h_{500.0\,m}$: Depth of 500.0 m bmsl.

h_{ss}: Sea surface

2.2.3. Kinetic behavior of gases

The gas speed determines the kinetic energy that gas could have. However, thermodynamically, the speed will depend on the gas temperatures. So, the kinetic behavior of several gases (R152a, R134a, ammonium, propane) will be studied to improve the efficiency of a thermal machine; using a computational process to model molecular speeds based on the kinetic theory of the gases, adapting Clausius theory and the data experiments of Graham (Garber, 2013). Because gas flux has three dimensions' molecular speeds, at a given temperature (T) (Anderson and Fenn, 1965), it is possible to determine the kinetic behavior of the fluid aslant average speed (v_{avg}), RMS (v_{rms}), and Most Probable speed (v_p).

2.2.4. Average speed, root mean square speed, and most probable speed

James Clerk Maxwell derives the most probable speed from determining how many gases molecules have a certain range of speeds (Halliday at al., 2011). The definition is a result of a distribution function, see Figure 2, through Equation 3:

$$v_{mp} = \sqrt{\frac{3 \cdot k_B \cdot T}{m}} \qquad \text{(Eq. 3)}$$

for average speed, Equation 4:

$$\overline{v} = \sqrt{\frac{8 \cdot k_B \cdot T}{\pi \cdot m}} \qquad \text{(Eq. 4)}$$

Figure 2. The speed distribution of gas

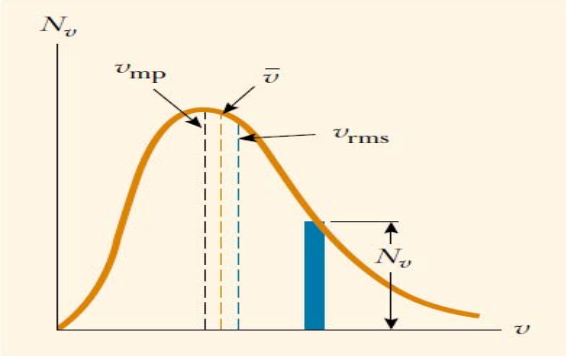

molecules at some temperature. Source: Fundamentals of Physics (p. 657) by Halliday, D. *et al.*., Jearl Walker.

And, for root mean square speed, Equation 5:

$$v_{rms} = \sqrt{\frac{2 \cdot k_B \cdot T}{m}} \qquad \text{(Eq. 5)}$$

where m is the mass of the gas, k_B is the Boltzmann's constant, and T is the absolute temperature.

3. RESULTS AND DISCUSSION:

3.1. Determining maximum efficiency in a thermal plant using thermal energy in the South American waters

More than 20% of the buoys processed (Pacific and Atlantic Oceans) stand out in the tropical waters around South America, achieving the maximum efficiency a machine could have from the two grids considered. The efficiency of the Carnot machine method, along the time since 1990, shows fluctuations increasing their amplitude from the coordinate 180º W of the Meridian Center (MC) line to the west, but the maxima value of efficiencies keeps invariable around 7.0% as 8º N 180º W, see Figure 3a. Minima values come down to 3.5% efficiency, mainly in the 0º N latitude of the Equator, as 0º N 95º W (see Figure 3b).

Taking a glance at the Atlantic Ocean, the smaller oscillations and major efficiencies are found in buoys located close to the Continent, as can be seen in Figure 4a, 4º N 38º W, with values around 6.5%, and Figure 4b, 0º N 35º W, rounding the 7.5% of efficiencies. While getting far from the

Downloaded from www.periodico.tchequimica.com

Continent, amplitudes of fluctuations increase considerably in time as 12º N 38º W, see Figure 4c.

It is notorious that better locations for installing thermal machines are placed in the Atlantic Ocean because of the proximity location of the buoys to the Continent. Nevertheless, small fluctuations might provide a stable machine in the Pacific Ocean, such as buoy 8º N 180º W. Although efficiencies of the outputs are smaller than 10%, it is necessary to know the energy intensity obtained from these waters to quantify these efficiencies.

However, thermal gradients present almost harmonically fluctuations in all the data sets (see Figure 5a, for buoy located at 2N 125W); but there is a buoy with anomaly values, 5º S 155º W, like 0.075 points, but the other values oscillate around 0.050 points, see Figure 5b. Thus, all of them are slightly affected by ENSO effects.

Observing thermal machine efficiencies analyzed in the PIRATA project, expected values oscillate periodically with uniform amplitudes such as buoy located at 15° N 38° W, see Figure 6a, but 23º W meridian such as buoy located at 12° N 23° W, see Figure 6b. These properties are opposite to the Pacific Ocean, where no dataset oscillates uniformly; their amplitudes of oscillations tend to diminish while moving off the Continent. All amplitudes of these buoys fluctuate randomly, but 2º S 140º W, where it is conceivable to acknowledge some enounced peaks, upward such as 1997, or downward such 1998, see Figure 7.

3.2. Study of thermal gradients around South America for implementation of thermal plants

Fluctuations of temperatures at the sea surface or at 500 m below the sea surface seem to oscillate periodically. However, periods might differ concerning each height, and the amplitude of oscillations varies considerably between buoys. Both matters make it improbable to stay in two reservoirs at fixed temperatures. There is a trend that temperatures decrease with time, but do amplitudes do it too? Comprehension of the time evolution of fluctuations of upper temperatures is essential because, undoubtedly, temperatures over the surface of tropical areas vary considerably, especially in the equatorial line.

In the Pacific Ocean, time series with major amplitudes of fluctuations are confined in the equatorial line (0º N) and at meridians closers to the Continent. Of course, amplitudes of oscillations of time series at 500 meters down the Ocean are prominently small, as the blue line in Figure 8a shows; but the trend is to vanish moving away from the equatorial line and move away at the north of the Continent, blue line in Figure 8b. Also, the red lines of Figure 8 show that fluctuations of temperatures at the sea surface have sizable amplitudes; then, both areas are unstable to install thermal plants in the Oceans.

In the Atlantic Ocean, fluctuations of temperatures at the Sea Surface and at 500-meter down are more stable than the buoys located on the other grid, above all, in the area closer to the Continent. This fact makes the Atlantic Ocean a proper place to install ocean thermal machines more feasible, especially in the South Hemisphere, until the 14º South from the equatorial line (see Figure 9).

In the Pacific Ocean, far away from the West of Quito, at North (8° N) and South (8° S), heftier gradients of temperatures with lesser amplitudes of oscillations of thermal gradients could be found, being these places stable zones (see Figure 10a). Near the seaboard of the Continent, in the latitude of 0º N (west of Quito, Equator), the amplitudes, which vary continuously, are the bigger of the two grids, attaining values around 0.025 ºC/m, making this area an unstable zone, see Figure 10b.

In the Atlantic Ocean, amplitudes are not as big as previous, but they are not small. It is possible to appreciate the maxima values of amplitudes arise at 0.04 ºC/m, in buoys far from the Continent, such buoy located at 0º N 23º W, see Figure 11a; and minima values are similar to those obtained in the Pacific Ocean, but only in two points, at 4º N 35º W and at 0º N 35º W, see Figure 11b. These last coordinates are optima places to install thermal machines.

3.3. Kinetic behavior of a fluid in a thermal turbine

A turbine rotor requires a driver gas within appropriate kinetic properties. On one side, their kinetic energy should be enough to run a turbine when the fluid converts into a gas at the Sea Surface. On the other side, the fluid at 500 meters bmsl ought to have a suitable speed to stay at the bottom. It is important to stay at the bottom. Then, it Is important to remember that fluid changes phase between 200 – 300 m depth, if kinetic energy increase uncontrolled, the fluid will have a trend to rising the surface.

Amplitudes of time series fluctuations of

Downloaded from www.periodico.tchequimica.com

every data set for root mean square, most probable speed, and average speed are extremely smalls; their values could be considered constants along the time. At 500 m bmsl, most probably speed, root mean square, and average speed has analogous values for every gas in every data set of both grids. R152a and R134a present the lowers values of speeds of 40 m/s. When the gas achieves the surface, most probable speeds obtain lower values of all kinds of speeds, especially from R152a, 250 m/s, and R134a, 220 m/s, as it is indicated in Figure 12a and Figure 12b, respectively. Propane and ammonium increase their values to 80 m/s and 120 m/s, respectively, at 500 m bmsl, and at the sea surface, they present higher values of these speeds, 660 m/s for ammonium, Figure 12a, and 420 m/s for propane, Figure 13b.

This fact implies that the first two gases (the artificial ones) and the last two (natural ones) will stay steady while the turbine is resting at 500 m bmsl. At Sea Surface, the major values of speeds are the averages, especially for ammonium, values of 660 m/s. So, it could be said that ammonium is the superior supplier for a rotor turbine, igniting fast, while R152a and R134a will increase kinetic energy little by little.

4. CONCLUSIONS:

This project has been realized to study the energy production obtained from the warmer waters around South America, which means temperature data of two points located in the same coordinates at different altitudes. Two methods were modeled for these daily data, the Carnot machine method on one side and thermal gradient on the other, including time series of each altitude and for each data set. The processes could be applied to any other grid with upper temperatures.

It has been seen that, during ENSO events, energy production increases several points for thermal gradients and Carnot Method, even though efficiencies are still low. Due to the fact that it is possible to supply turbines with an adequate gas to obtain energy around these waters, three kinds of speeds were modeled average speed, root means square, and the most probable speed for four gases, just R152a, R134a, propane, and mainly ammonium.

At the west of Canal (8° N, 125° W) of Panama and Huanchaco (Trujillo) (8° S, 125° W), it could find the most suitable areas to install thermal machines. The weaker areas are located around Quito, Equator, because of fluctuations of the magnitudes of the gradients. The closest place to install these machines in South America is North of Brazil at the East of Sâo José de Macapá (0° N, 35° W) and East of French Guyana (4° N, 35° W).

Graphically, it has been seen that ammonium speeds were higher for both depths, at the sea surface and 500 m bmsl, followed by propane with comparable speeds. But R152a and R134a have lower speeds at 500 m down the Ocean and at the sea surface, much smaller than previous. Also, it has been seen that the smaller amplitudes of fluctuations of Carnot efficiency and thermal gradients are found in the Atlantic Ocean, near the French Guiana (4º N 38º W); and in the Pacific Ocean in the latitudes of Panama (8º N 125º W) and the 8º S 125º W, in the Peruvian latitudes.

5. DECLARATIONS:

5.1. Study Limitations

The study is limited to the sample analyzed.

5.2. Acknowledgements

This project was made with the support of the Facultad de Ciencias of Universidad Nacional de Ingeniería, and Facultad de Ingeniería Ambiental, Centro de Tecnoligías de la Información y Comunicaciones (CTIC-UNI) of Universidad Nacional de Ingeniería, and Clever for their cooperation on this Project. Also, the cooperation of Manuel Chirinos Coya (Heald College – Independent worker) and Raul Chirinos Coya (California State University, East Bay – Senior Software Developer) were determined to develop the programs to process the data for PMEL-NOAA.

Thanks to my family Teresa Chirinos, Teresa Díez, Miriam Loayza, Abbie Diez, and Paul Díez, for enabling me to keep working on this project.

5.3. Funding source

"This research was funded by the authors and by the Facultad de Ingeniería Ambiental of Universidad Nacional de Ingeniería".

5.4. Competing Interests

None.

5.5. Open Access

This article is licensed under a Creative Commons Attribution 4.0 (CC BY 4.0) International License, which permits use, sharing,

adaptation, distribution, and reproduction in any medium or format, as long as you give appropriate credit to the original author(s) and the source, provide a link to the Creative Commons license, and indicate if changes were made. The images or other third-party material in this article are included in the article's Creative Commons license unless indicated otherwise in a credit line to the material. If material is not included in the article's Creative Commons license and your intended use is not permitted by statutory regulation or exceeds the permitted use, you will need to obtain permission directly from the copyright holder. To view a copy of this license, visit http://creativecommons.org/licenses/by/4.0/.

6. REFERENCES:

1. Anderson, J. B. and Fenn, J. B. (1965). Velocity Distribution in Molecular Beams from Nozzle Sources. AIP Physics of Fluids, (8): 780-787.

2. Bernardoni, C., Binotti, M. and Giostri A. (2019). Techno-economic analysis of closed OTEC cycles for power generation. Renewable Energy, 132: 1018-1033.

3. Center for Weather Forecasting and Climate Studies. National Institute for Space Research. Repositorio GOES 16. http://satelite.cptec.inpe.br/repositoriogoes/goes16/goes16_web/gl_sat_rgb_baixa/2018/12/S11635397_201812171445.jpg.

4. Cronin, M. F., and McPhaden, M. J., The upper ocean heat balance in the western equatorial Pacific warm pool during September-December 1992. (1997). Journal of Geophysical Research, 21: 8533-8553.

5. Damy, G. and Marvaldi J. (1987). Some Investigations on the Possibility of using Ocean Thermal Gradient (OTG) for seawater desalination. Institute Français de Recherche pour l'Explotation de la Mar (IFREMER), 18: 197-214.

6. Emery, W. J., Pickard, G. L. (2007). Descriptive Physical oceanography. Academic Press, Elsevier, San Diego, CA.

7. Etemadi, A., Emdadi A., Afshar, O. A., Emami, Y., Goncalves I. B. and Molander S. (2017). Electricity Generation by the Ocean Thermal Energy. Energy Procedia, 8: 178-185.

8. Faizal, M. and Ahmed, M.R. (2017). Experimental studies on a closed cycle demonstration OTEC plant working on small temperature difference. Renewable Energy, 7: 234-240.

9. Garber, E.W. (1970). Clausius and Maxwell's Kineti Theory of gases. Historical Studies in the Physical Sciences, 21: 299-319.

10. Halliday, D., Resnick, R. and Walker, J. (2011). Fundamentals of Physics. Jefferson City, MO.

11. Hammar, L., Gullström, M., Dahlgren, T. G., Asplund, M. E., Goncalves, I. B. and Molander, S. (2017). Introducing ocean energy industries to a busy marine environment. Renewable and Sustainable Energy Reviews, 8: 178-185.

12. Harrison, D. E. and Craig, A. P. (1992). Ocean Models Studies of Upper-Ocean Variability at 0º, 160º W during the 1982-1983 ENSO: Local and Remotely Forced Response. Journal of Physical Oceanography, 26: 425-450.

13. Johnson, G. C., Solyan, B. M., Kessler, W. S. and McTaggart, K. E. (2002). Direct measurements of upper ocean currents and water properties across the tropical Pacific during the 1990s, 52: 31-61.

14. Johnson, G. C., Mecking, S., Solyan, B. M. and Wijffels, S. E. (2007). Recent Bottom Water Warming in the Pacific Ocean. Journal of Climate, 11: 5365-5375.

15. Lymann, J. M., Johnson and G. C. (2013). Estimating Global Ocean Heat Content Changes in the Upper 1800 m since 1950 and the Influence of Climatology Choice. Journal of climate, 13: 1945-1957.

16. Meinen, C. S. and McPhaden, M. J., Observations of Warm Water Volume Changes in the Equatorial Pacific and Their Relationship to El Niño and La Niña.

Downloaded from www.periodico.tchequimica.com

(2000). Journal of climate, 9: 3551-3559.

17. McPhaden, M. J. and Hayes, S. P. (1991). On the Variability of Winds, Sea Surface Temperature, and Surface Layer Heat Content in the Western Equatorial pacific. Journal of Geophysical Research, VOL 96, 12: 3331-3342.

18. McPhaden, M. J., Zebiak, S. E. and Glantz, M. H. (2006) ENSO as an integrating Concept in Earth Science. Science, 6: 1740-1745.

19. McPhaden, M. J., Timmermann, A., Widlansky, M. J., Balmaseda, M. A., and Stockdale, T. N. (2015). The curious case of the El Niño that never happened. Bulletin of the American Meteorological Society, 19: 1647-1665.

20. Miller, R. C. and Kusch, P. (1965). Velocity Distribution in Potassium and Thallium Atomic Beams. Physical Review, 8: 1314-11321.

21. O'Donovan, T.. S. and Murray, D. B. (2007). Jet impingement heat transfer – part I: Mean and root-mean-square heat transfer and velocity distributions. International Journal of Heat and Mass Transfer, 11: 3292-3301.

22. PMEL-NOAA [https://www.pmel.noaa.gov/gtmba/]. Orlando. Global Marine Buoy Array. [Cited May 2019]. Available from: https://www.pmel.noaa.gov/tao/drupal/disdel/.

23. Purkey, S. G., Johnson and G. C. (2010). Warming of Global Abyssal and Deep Southern Ocean Waters between the 1990s and 2000s: Contribution to Global Heat and Sea Level Rise Budgets. Journal of Climate, 16: 6336-6351.

24. Rebhan, E. (2002). Efficiency of nonideal Carnot engines with friction and heat losses. American Journal of Physics, 8: 1143-1150.

25. Resurreiçao, A., Gibbons, T. P., Dentinho, T. P., Kaiser, M., Santos, R. S., and Edwards-Jones, G. (2011). Economic valuation of species loss in the open sea. Ecological Economics, 11: 729-739.

26. Salam, M. A. and Khan, A. S. (2017). Transition towards sustainable energy production – A review of the progress for solar energy in Saudi Arabia. Energy Exploration and Exploitation, 9: 6-14.

27. Semmari, H., Sittou, D. and Mauran, S. (2012). A novel Carnot-based cycle for ocean thermal energy conversion. Energy, 15: 361-375.

28. Singh, A. (2013). A simplistic pedagogical formulation of a thermal speed distribution using relativistic framework. Journal of Physics, 14: 143-156.

29. Technische Universiteit Delft (2021, October, 20) TuDelft. Retrieved from https://www.tudelft.nl/oceanenergy/research/thermal-gradient-otec/.

30. Wolfe, E. (2013). Clausius and Maxwell's Kinetic Theory of Gases. Historical Studies in the Physical Sciences, 21: 299-319.

Downloaded from www.periodico.tchequimica.com

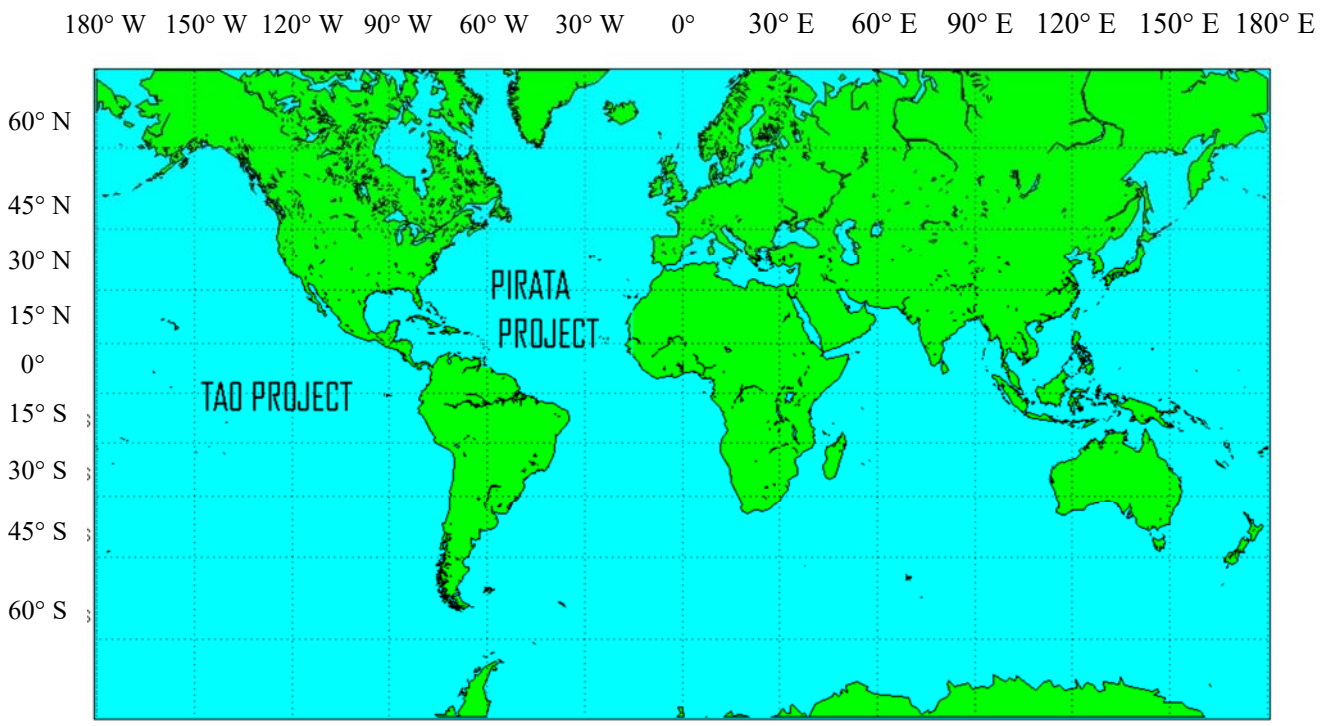

Figure 1. *Grids of the TAO/TRITON and PIRATA projects of PMEL-NOAA, inside the geographical coordinates (0° N, 180° W), (8° S, 180° W), (0° N, 95° W), and (8° S, 95° W) in the Pacific Ocean; and, inside the geographical coordinates (20° N, 35° W), (8° N, 38° W), (21° N, 23° W), and (12° N, 23° W), in the Atlantic Ocean. Adapted: Matlab 2009a Student version.*

Downloaded from www.periodico.tchequimica.com

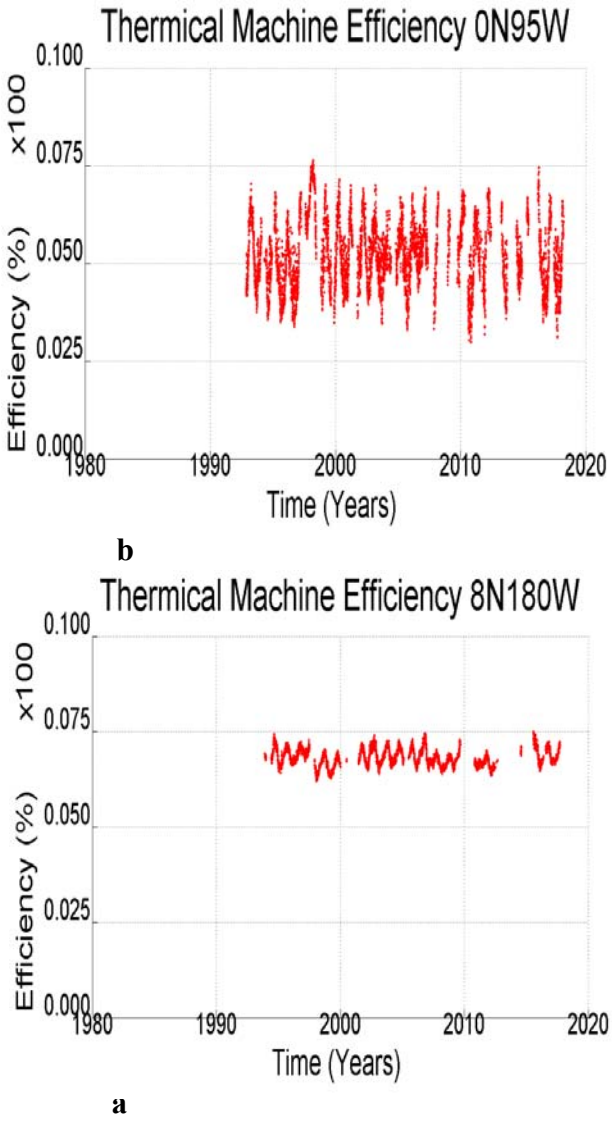

Figure 3. *Carnot machine efficiencies modeled by two reservoirs at the Sea Surface and up 500 m bmsl, in the Pacific Ocean at 8º N 180º (a) and 0º N 95º W (b).*

Downloaded from www.periodico.tchequimica.com

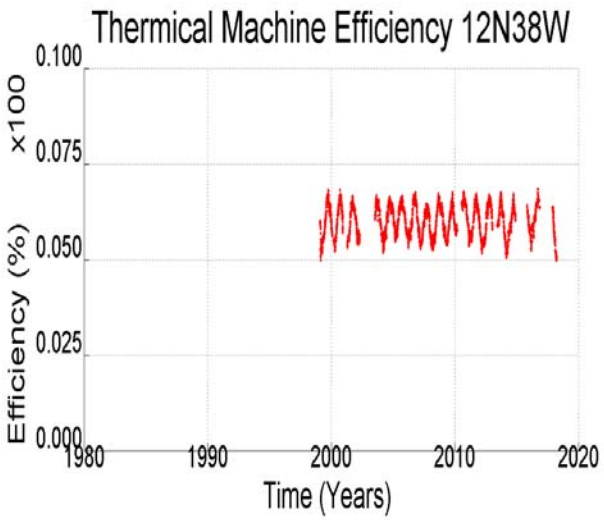

c

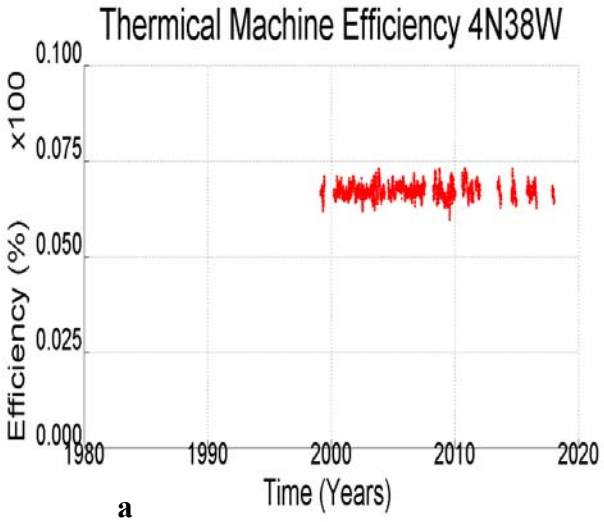

a

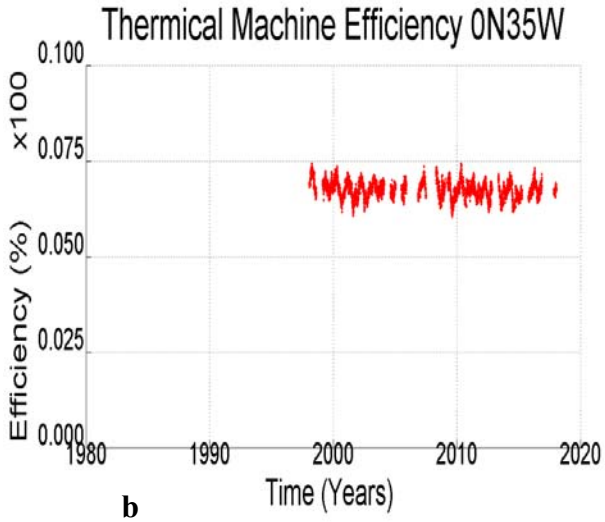

b

Figure 4. *Carnot machine efficiencies modeled by two reservoirs at sea surface and up 500 m bmsl, in the Atlantic Ocean at 4º N 38º (a), 0º N 35º W (b) and 12º N 38º W (c).*

Downloaded from www.periodico.tchequimica.com

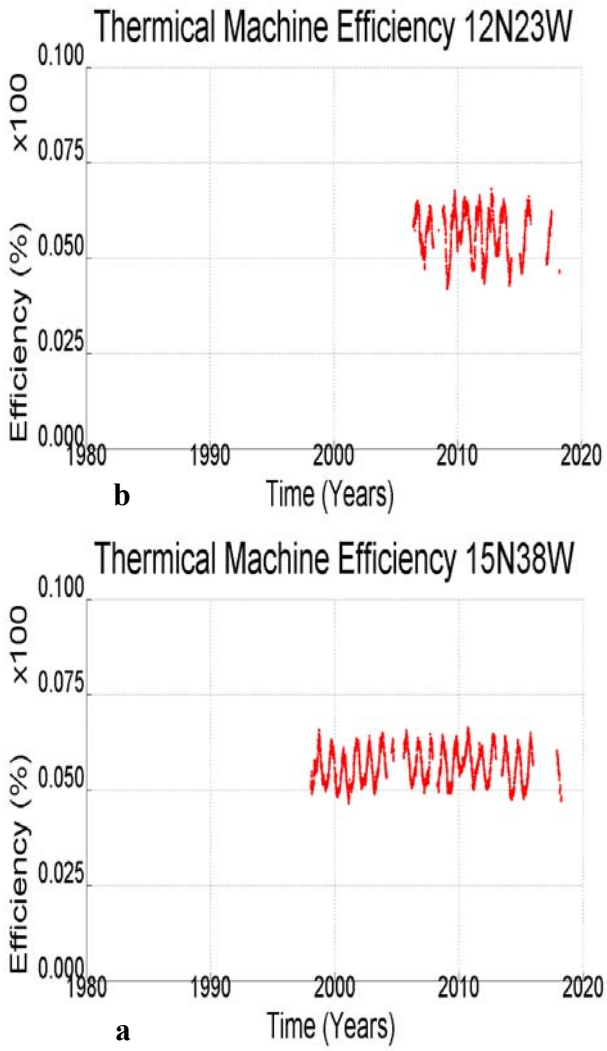

Figure 5. *Fluctuations of thermal gradients for a buoy located at 2º N 125º W (a) and 5º S 155º W (b).*

Downloaded from www.periodico.tchequimica.com

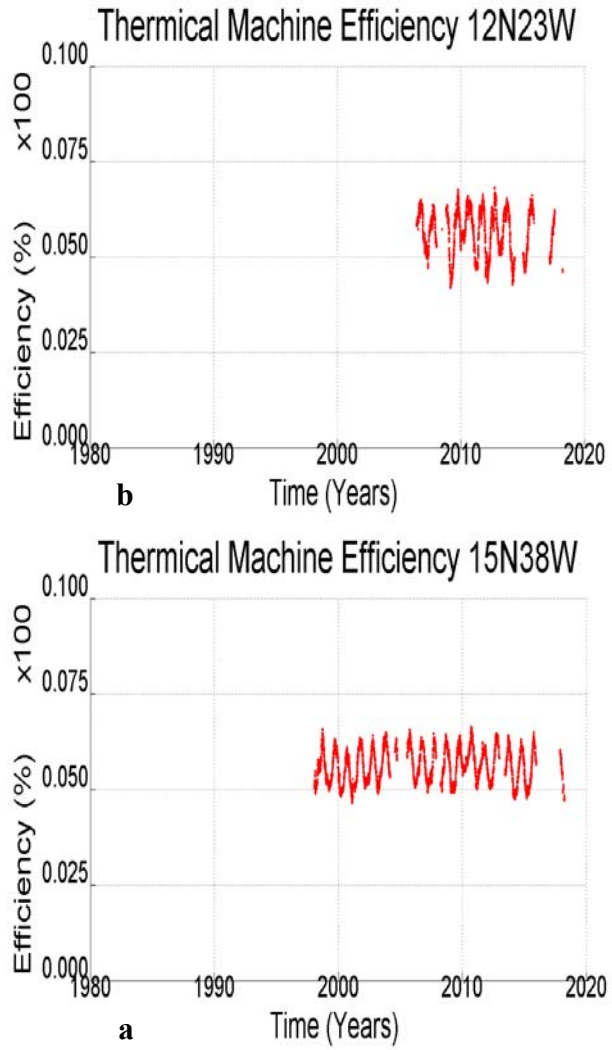

Figure 6. *Carnot efficiencies for buoys located: outside the 38º W meridian (15º N 38º W) (a) and inside the 23º W meridian (12º N 23º W) (b).*

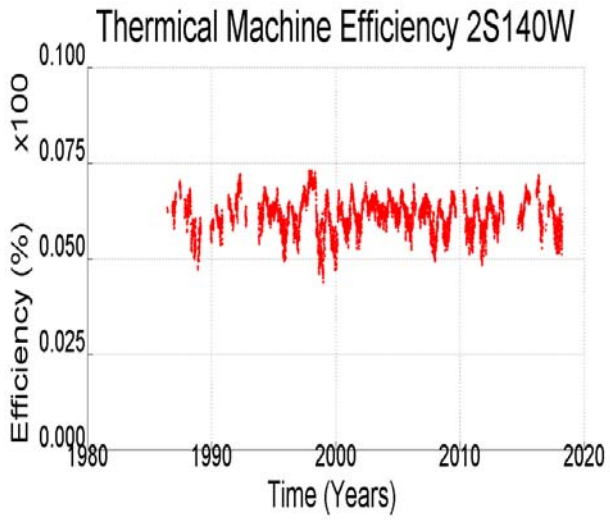

Figure 7. Carnot efficiency for a buoy that is located at 2º S 140º W, where appears peaks upward and downward, related to several ENSO events.

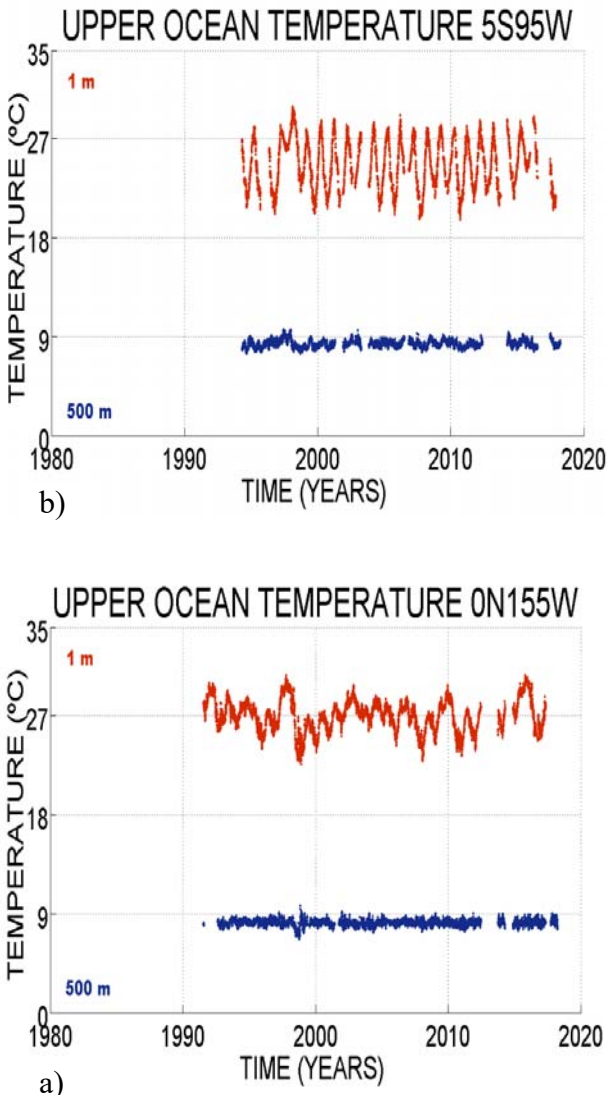

Figure 8. *Time series of temperatures at the sea surface (red line) and up 500 m. bmsl (blue line) in the Pacific Ocean at 0º N 155º W (a) and at 5º S 95º W (b).*

Downloaded from www.periodico.tchequimica.com

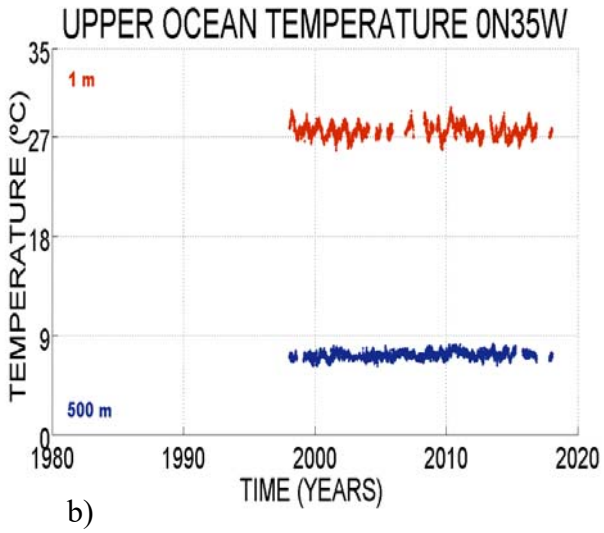

b)

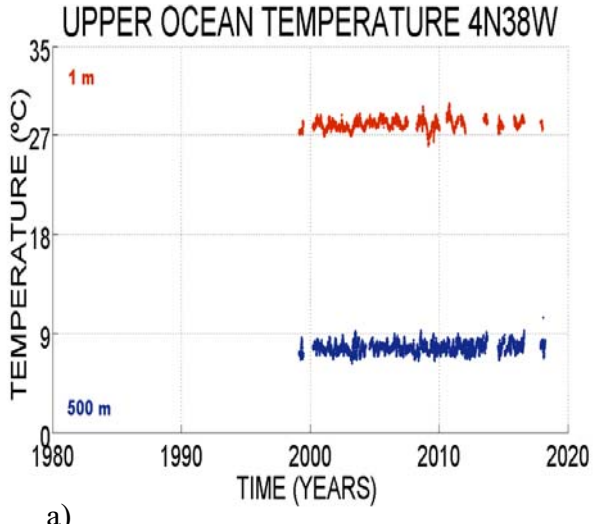

a)

Figure 9. *Time series of temperatures at sea surface (red line) and up 500 m. bmsl (blue line) in the Atlantic Ocean at 0º N 35º W (a) and at 4º N 38º W (b).*

Downloaded from www.periodico.tchequimica.com

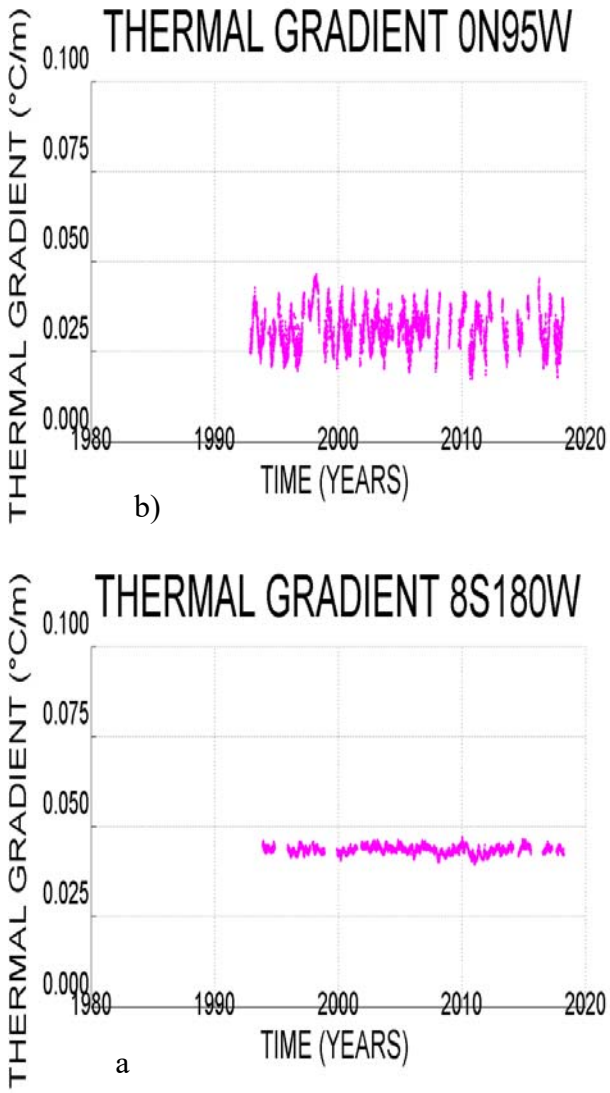

Figure 10. *Time series of gradients of temperatures at sea surface and up 500 m. bmsl in the Pacific Ocean at 8º S 180º W (a) and at 0º N 95º W (b).*

Downloaded from www.periodico.tchequimica.com

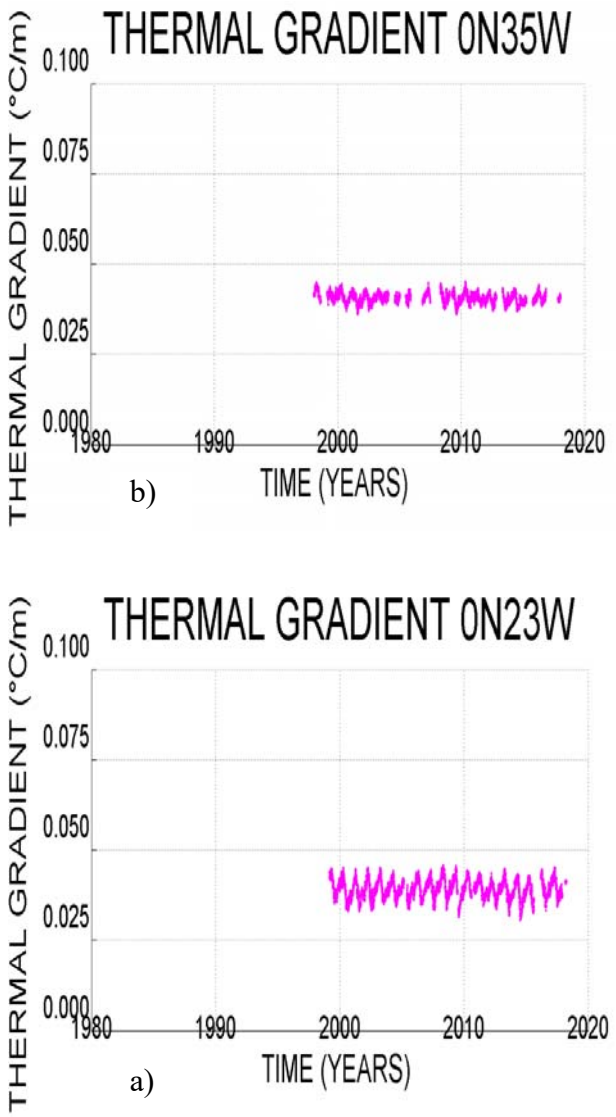

Figure 11. *Time series of gradients of temperatures at sea surface and up 500 m. bmsl in the Atlantic Ocean at 0º N 23 º W (a) and at 0º N 35º W (b).*

Downloaded from www.periodico.tchequimica.com

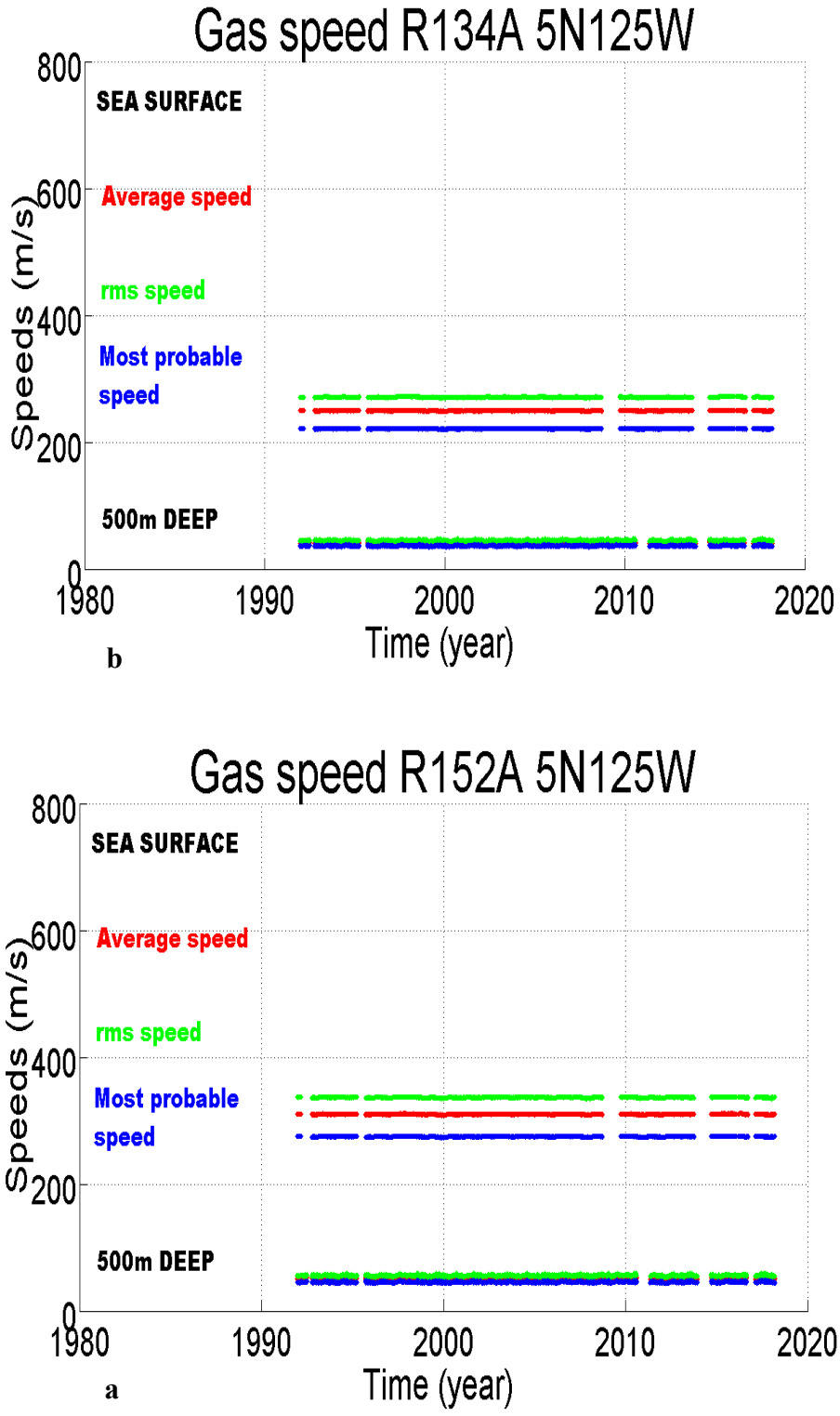

Figure 12. *Gas speed respect time evolution, at the sea surface (on top) and at 500 m bmsl (on the bottom), red line, average speed; green line, RMS; and blue line, Most Probable speed, for the latitude of 5º N and meridian of 125º W for R152a (a) and R134a (b).*

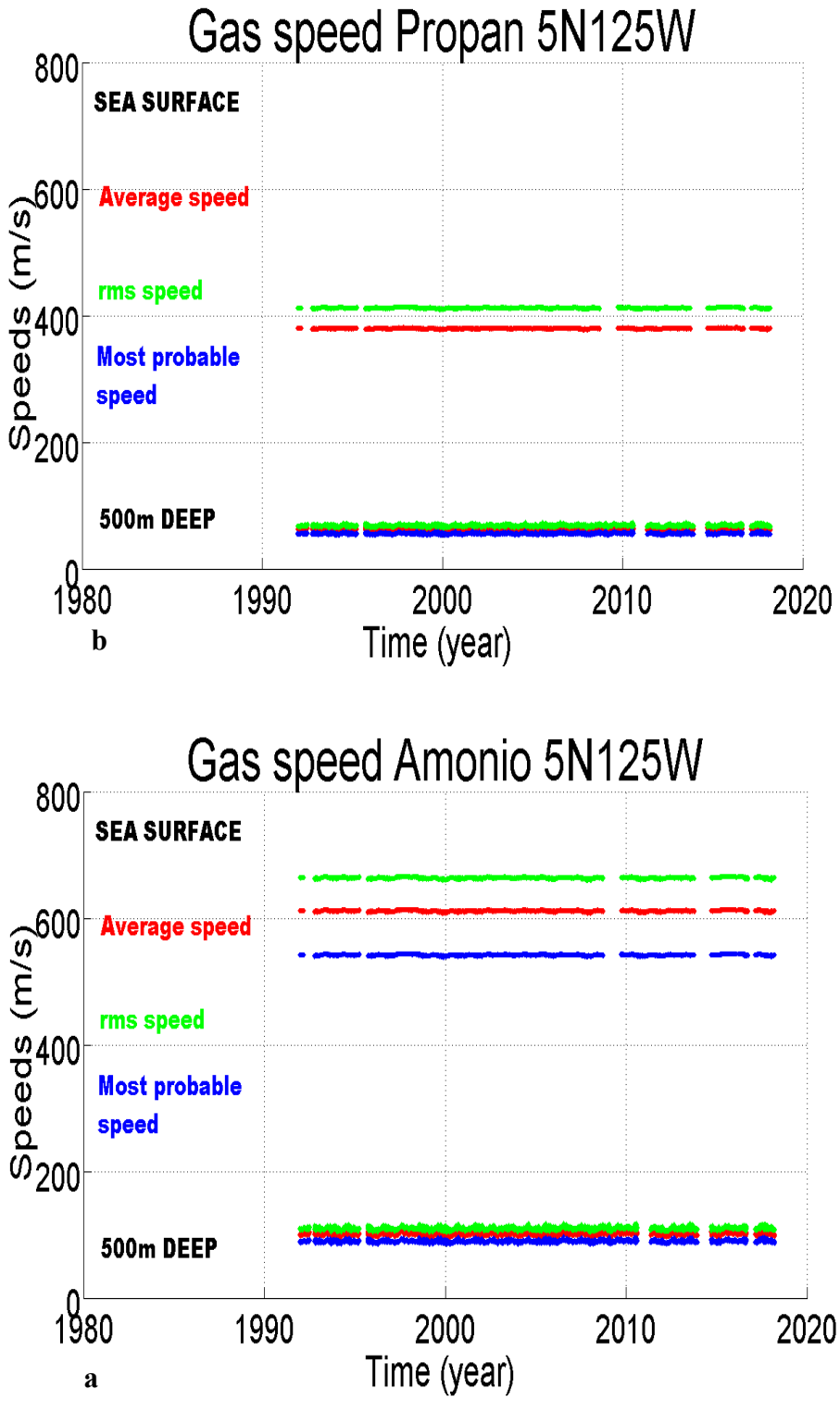

Figure 13. *Gas speed respect time evolution, at the sea surface (on top) and at 500 m bmsl (on the bottom), red line, average speed; green line, RMS; and blue line, Most Probable speed, for the latitude of 5º N and meridian of 125º W for Ammonium (a) and propane (b).*

Downloaded from www.periodico.tchequimica.com